### Title

A Combinatorial Library of Biodegradable Polyesters Enables Non-viral Gene Delivery to Post-Mitotic Human Stem Cell-Derived Polarized RPE Monolayers




### Journal

Regenerative Engineering and Translational Medicine, 6(3)

### ISSN

2364-4133



### Authors

Mishra, Bibhudatta
Wilson, David R
Sripathi, Srinivas R
et al.



### Publication Date

2020-09-01

### DOI

10.1007/s40883-019-00118-1

HHS Public Access

Author manuscript

*Regen Eng Transl Med*. Author manuscript; available in PMC 2021 March 16.

Published in final edited form as:

*Regen Eng Transl Med*. 2019 September ; 6(3): 273–285. doi:10.1007/s40883-019-00118-1.

# A combinatorial library of biodegradable polyesters enables non-viral gene delivery to post-mitotic human stem cell-derived polarized RPE monolayers

**Bibhudatta Mishra**[1,Φ], **David R. Wilson**[2,3,4,Φ], **Srinivas R. Sripathi**[1], **Mark P. Suprenant**[2,3], **Yuan Rui**[1,2,3], **Karl J. Wahlin**[1,$], **Cynthia A. Berlinicke**[1], **Jordan J. Green**[1,2,3,4,6,7,8,*], **Donald J. Zack**[4,5,9,10,11,*]

[1]Ophthalmology, Johns Hopkins University School of Medicine, Baltimore, MD 21231, United States

[2]Biomedical Engineering, Johns Hopkins University, Baltimore, 21231, United States

[3]Translational Tissue Engineering Center, Johns Hopkins of Medicine, Baltimore, MD 21231, United States

[4]Institute for Nanobiotechnology, Johns Hopkins University, Baltimore, MD 21231, United States

[5]Neuroscience, Johns Hopkins University School of Medicine, Baltimore, MD 21231, United States

[6]Oncology, Johns Hopkins University School of Medicine, Baltimore, MD 21231, United States

[7]Materials Science and Engineering, Johns Hopkins University, Baltimore, MD 21231, United States

[8]Neurosurgery, Johns Hopkins University School of Medicine, Baltimore, MD 21231, United States

[9]Molecular Biology and Genetics, Johns Hopkins University School of Medicine, Baltimore, MD 21231, United States

[10]Neuroscience, Johns Hopkins University School of Medicine, Baltimore, MD 21231, United States

[*]To whom correspondence should be addressed: Jordan J. Green, green@jhu.edu, Donald J. Zack, dzack@jhmi.edu.
[$]Current Address: Shiley Eye Institute, University of California San Diego, La Jolla, California USA
[Φ]These authors contributed equally to this work

AUTHOR CONTRIBUTION

Overall conceptualization, B.M., D.R.W., D.J.Z and J.J.G; Methodology and Investigation, B.M., D.R.W., S.S.R, M.P.S., C.B., and Y.R.; Resource Generation (plasmid DNA designing and production), K.J.W., (stem cell differentiation and maintenance), S.S.R.; Writing—Original Draft, B.M., D.R.W., C.B., D.J.Z and J.J.G ; Writing—Review & Editing, B.M., D.R.W., C.B., D.J.Z and J.J.G.; Funding Acquisition, D.J.Z., J.J.G., S.S.R., D.R.W., and Y.R. ; Supervision and Project Administration, D.J.Z and J.J.G.



CONFLICT OF INTEREST STATEMENT

DJZ is on the scientific advisory board of Spark Therapeutics, which is interested in developing optimized approaches for retinal gene delivery.

[11]Institute of Genetic Medicine, Johns Hopkins University School of Medicine, Baltimore, MD 21231, United States

## Abstract

Safe and effective delivery of DNA to post-mitotic cells, especially highly differentiated cells, remains a challenge despite significant progress in the development of gene delivery tools. Biodegradable polymeric nanoparticles (NPs) offer an array of advantages for gene delivery over viral vectors due to improved safety, carrying capacity, ease of manufacture, and cell-type specificity. Here we demonstrate the use of a high-throughput screening (HTS) platform to synthesize and screen a library of 148 biodegradable polymeric nanoparticles, successfully identifying structures that enable efficient transfection of human pluripotent stem cell differentiated human retinal pigment epithelial (RPE) cells with minimal toxicity. These NPs can deliver plasmid DNA (pDNA) to RPE monolayers more efficiently than leading commercially available transfection reagents. Novel synthetic polymers are described that enable high efficacy non-viral gene delivery to hard-to-transfect polarized human RPE monolayers, enabling gene loss- and gain-of-function studies of cell signaling, developmental, and disease-related pathways. One new synthetic polymer in particular, 3,3′-iminobis(N,N-dimethylpropylamine)-end terminated poly(1,5-pentanediol diacrylate-co-3 amino-1-propanol) (5-3-J12), was found to form self-assembled nanoparticles when mixed with plasmid DNA that transfect a majority of these human post-mitotic cells with minimal cytotoxicity. The platform described here can be utilized as an enabling technology for gene transfer to human primary and stem cell-derived cells, which are often fragile and resistant to conventional gene transfer approaches.

## Lay Summary:

Many retinal diseases are attributable to dysregulation in gene expression or lack of expression of specific genes, allowing for the possibility of prevention or cure of these diseases by effective delivery of nucleic acids coding for the necessary gene to the retina. Delivery of nucleic acids to cells of the retina is challenging due to the non-dividing nature of most retinal cells, preventing DNA from reaching the nucleus. To overcome this barrier, we engineered and tested a library of nanoparticle formulations to identify polymers that enabled safe and effective delivery of nucleic acid cargoes to retinal pigment epithelial cells. The nanoparticle technology explored here has the potential to be utilized for therapeutic delivery of nucleic acids to retinal cells, possibly enabling treatment for otherwise untreatable retinal diseases for which a specific genetic deficit is known but no drugs are available.

### Keywords

Retinal pigment epithelial cell; human stem cell; nanoparticles; non-viral gene therapy; poly(beta-amino ester); polymer; ophthalmology

## 1. INTRODUCTION:

Gene therapy holds promise for treating many acquired and inherited blinding disorders [1]. Gene therapy for long-term expression, particularly *in vivo,* has traditionally utilized viral

vectors to deliver double stranded DNA. For retinal gene therapy, adeno-associated virus (AAV) in particular has been successfully utilized for effective delivery to various cells of the retina [2]. However, utilization of AAV vectors for gene therapy does have a number of drawbacks, including limited cargo capacity of the AAV capsid [3–5], risk of insertional mutagenesis [6], the challenge of large scale production of clinical grade vector for human therapy [7], difficulty in transducing some cell types, and as pre-existing patient immunity to specific AAV serotypes [2, 8]. To overcome these challenges and to develop a potentially safer approach, an alternative strategy that is receiving increased attention is the formulation and development of biodegradable non-viral vectors to facilitate delivery of the gene of interest to the target site of interest. Non-viral vectors, although they have their own challenges such as relatively low efficiency, have the potential to overcome many of the drawbacks of AAV and other viral-based gene delivery methods [9].

With this goal of developing safe and efficient non-viral methods for gene delivery, a wide variety of non-viral nanoparticles (NPs) have been engineered and tested [10–16]. NPs have been developed that can effectively complex with nucleic acids, mediate cell uptake, achieve endosomal escape, and result in cellular gene expression. However, despite these significant successes, DNA transfecting NPs that have been developed to date have tended to suffer from low efficacy [17]. Efficacy of non-viral transfection reagents in post-mitotic cell types that have exited the cell cycle is particularly low, as nuclear uptake of plasmid DNA remains a major hurdle to effectively mediating expression [18, 19]. Poly(beta-amino ester)s (PBAEs) are a promising class of synthetic, cationic polymers with large structural diversity that have been demonstrated to effectively condense plasmid DNA into nanoparticles via electrostatic interactions and self-assembly, and to transfect a wide variety of cells including embryonic stem cells [20], as well as immortalized human RPE cell lines *in vitro* and mouse RPE cells *in vivo* [21].

The RPE, which is essential for retinal function, is composed of a monolayer of pigmented bipolar epithelial cells at the backside of the retina. Compromise of the cellular environment of the RPE is associated with many hereditary and acquired retinal diseases, including age-related macular degeneration (AMD) and retinitis pigmentosa (RP) [22]. Mutations of genes expressed in the RPE are associated with a number of retina diseases, and viral-based gene therapies are actively being pursued for several of these diseases [23]. In fact, the first FDA approved gene therapy for an inherited disease (voretigene neparvovec-rzyl) is for an RPE-related disease, using an AAV-based vector system. Building upon this success, a number of academic and industry groups are pursuing gene therapies for a number of other RPE-related genetic diseases. A challenge in this work is that a number of the diseases of interest involve genes that exceed the limited carrying capacity of AAV. One approach to address this challenge involves clever efforts to artificially increase AAV's carrying capacity [24] A second approach involves efforts to develop other classes of viral gene vectors for retinal disease [25, 26]. A third approach, as noted above, involves development of non-viral approaches. However, despite the testing of many different non-viral strategies to deliver DNA to RPE, the success of the technologies that have been tested to date has been limited [27–36]. To address this challenge, we first established a high throughput-assay platform to screen potential PBAE nanoparticles for their ability to efficiently transfect iPSC-derived human RPE monolayers *in vitro*. Additionally, we hypothesized that the efficiency of

cationic PBAE-pDNA NPs to transduce RPE monolayers could be significantly increased by tuning the hydrophilicity and end group chemistry of the constituent polymers. To test this hypothesis, we synthesized 4 PBAE base polymers with different backbones and then end-capped the linear polymers in a parallel plate-based format to yield a library of 148 polymer structures. This library of polymers, that included novel amine-containing small molecules as end-groups to serve as putative transfection enhancers, was then screened using the high throughput human iPSC RPE monolayer assay. Here we describe identification of several promising NPs for RPE transfection.

## 2. MATERIALS AND METHODS:

### 2.1 Polymer synthesis and characterization

Monomers for base polymer synthesis were purchased from vendors listed in Table S2, while end-cap monomers used were purchased from vendors listed in Table S3 and S4. Acrylate monomers were stored with desiccant at 4°C, while amine monomers were stored with desiccant at room temperature. PBAE polymers were synthesized neat at 1.1:1 B:S monomer ratios for polymers 3-5-Ac, 4-4-Ac and 4-5-Ac and 1:1.05 monomer ratio for 5-3-Ac for 24 hours at 90°C. Following synthesis, neat polymers were dissolved at 200 mg/mL in anhydrous DMF then precipitated in diethyl ether twice at a solvent ratio of 1:10 by vortexing the solvents and centrifuging at 3000 rcf. Polymers were allowed to dry under vacuum for 24 hours, at which point they were massed and dissolved at 200 mg/mL in anhydrous DMSO and allowed to remain under vacuum to remove additional diethyl ether for another 24 hours. Finally, acrylate terminated polymers were aliquoted and stored at −20°C until use in end capping reactions.

For polymer characterization, samples of the initial neat polymer and neat polymer following diethyl ether removal were set aside for characterization via $^{1}$H NMR and gel permeation chromatography (GPC). GPC was performed on polymer samples both before and after double precipitation in diethyl ether using a Waters system with auto sampler, styragel column and refractive index detector to determine $M_N$, $M_W$ and PDI relative to linear polystyrene standards. GPC measurements were performed as previously described with minor changes consisting of a modified flow rate (0.5 mL/min) and an increase in sample run time to 75 minutes per sample[37]. Analysis of polymers via $^{1}$H NMR (Bruker 500 MHz) following diethyl ether precipitation and drying was performed to confirm the presence of acrylate peaks. For NMR, neat polymer was dissolved in $CDCl_3$ containing 0.05% v/v tetramethylsilane (TMS) as an internal standard.

### 2.2 Polymer library preparation

PBAE polymers were prepared for transfection screening experiments by high-throughput, semi-automated synthesis techniques using a ViaFlo 384 (Figure 2B). For end capping reactions, 25 μL of end-cap molecules in anhydrous DMSO at a concentration of 0.2 M were distributed to source wells of a deep-well 384 well plate, then distributed to corresponding replicate wells in groups shown in multiple colors of the end capping reaction 384-well deep plate (240 μL volume). Acrylate terminated base polymers at 200 mg/mL in anhydrous DMSO were thawed and distributed to wells containing 36 different end-cap molecules and

a single well containing DMSO only for the acrylate terminated polymer control. End capping reactions were allowed to proceed for two hours at room temperature on a gentle shaker, after which end-capped PBAE polymers were diluted to 50 mg/mL in anhydrous DMSO and aliquoted to 5 μL per well on the left side of 384-well nanoparticle source plates. Nanoparticle source plates were sealed and stored at −20°C with desiccant until needed for transfection. Following large-scale screening of the PBAE library in 384-well plates, larger batches of top PBAE structures were synthesized from frozen base polymer using the same protocol described above. End-capped polymers were then aliquoted to individual tubes and stored at −20°C with desiccant.

For end capping, reaction volumes of 50 μL at 100 mg/mL polymer concentration and 0.1 M amine monomer end-cap concentration were selected as sufficient to enable effective reactivity over a two-hour time period. For initial studies, end-cap molecule E1 was titrated between 0.2 and 0.0625 M in reactions with base polymer PBAE 4-5-Ac at 100 mg/mL over two hours. Reacted polymers were then precipitated twice in diethyl ether to remove excess end-cap monomer, dried and assessed using 1H NMR to determine efficacy of the end capping reaction by the disappearance of acrylate moiety peaks between 5.5–6.5 ppm. These results demonstrated effective end capping down to a concentration of 0.05 M for end-cap molecule E1. To allow for varying levels of reactivity between end-cap molecules, an end-cap molecule concentration of 0.1 M was used for parallel large-scale end capping reactions.

### 2.3 Differentiation and Culture of RPE From hPSCs

RPE monolayers were differentiated as described previously [38, 39] from the EP1-GFP human iPS cell line that constitutively expresses H2B-nuclear-GFP. In brief, iPS cells to be differentiated were plated at 60,000 cells per $cm^2$ on Matrigel-coated 384-well plates and allowed to grow for 25 days in RPE medium consisting of 70% DMEM (catalog no. 11965092; ThermoFisher Scientific), 30% Ham's F-12[40] Nutrient Mix (catalog no. 11765–054; Invitrogen), serum free B27 supplement (catalog no. 17504044; ThermoFisher Scientific), and antibiotic-antimycotic (catalog no. 15240062; ThermoFisher Scientific). Coating of plates with Matrigel (25 μL per well), seeding of cells (50 μL per well), and media change every other day (replaced with fresh 25 μL per well) were accomplished using a high throughput Viaflo microplate dispenser (catalog no. 6031; Intergra). Cells were confirmed to possess an RPE monolayer phenotype at day 25 following plating.

### 2.4 Nanoparticle characterization

Following transfection screening, 5-3-J12 polymer was selected as the top performer due to it's high transfection efficacy and robustness. The hydrodynamic diameter of top PBAE structure 3,3′-iminobis(N,N-dimethylpropylamine)-end terminated poly(1,5-pentanediol diacrylate-co-3 amino-1-propanol) (5-3-J12) was characterized at three different w/w ratios to assess the influence of w/w ratio on nanoparticle characteristics. For dynamic light scatter (DLS) measurements, nanoparticles were initially formed in 25 mM $MgAc_2$, pH 5.0 then diluted 1:6 into 10% FBS in PBS dynamics and analyzed in disposable micro-cuvettes using a Malvern Zetasizer NanoZS (Malvern Instruments, Malvern, UK) with a detection angle of 173°. For zeta potential, nanoparticles were prepared and diluted as for DLS, but were analyzed by electrophoretic light scattering was in disposable zeta cuvettes at 25°C using the

same Malvern Zetasizer NanoZS. For nanoparticle tracking analysis, nanoparticles were formed in 25 mM $MgAc_2$, pH 5, then diluted 1:500 in 150 mM PBS as previously described using a Nanosight NS300 [41].

A gel retention assay to assess PBAE: DNA binding strength was performed as previously described [42] using a 1% agarose gel. Acrylate terminated PBAE 5-3-Ac was compared against top PBAE structure 5-3-J12 at w/w ratios from 0 to 50 to demonstrate improved binding of end-capped PBAE structures.

Transmission electron microscopy (TEM) images were acquired using a Philips CM120 (Philips Research, BriarcliffsManor, New York) on 400 square mesh carbon coated TEM grids. Samples were prepared at a DNA concentration of 0.045 μg/μL and polymer 90 w/w ratio in 25 mM $MgAc_2$, pH 5.0 after which 30 μL were allowed to coat TEM grids for 20 minutes. Grids were then dipped briefly in ultrapure water, wicked dry and allowed to fully dry before imaging.

### 2.5 Plasmid Design

For the *in vitro* transfection, a plasmid coding for the mCherry open reading frame was created by PCR amplification of the mCherry-N1 plasmid (catalog no. 632523; Clontech). Since this plasmid has no start site, an ATG initiation codon was added to the forward primer. After PCR amplification, mCherry was inserted into the directional pENTR-D-TOPO gateway entry vector (catalog no. K240020; Invitrogen). Positive colonies were selected by PCR and confirmed by sequencing. 100ng of purified entry plasmid was mixed with pCAGG-DV destination vector, created by incorporating a gateway cassette containing attR recombination sites flanking a ccdB gene into the pCAGEN vector (Addgene #11160), in the presence of LR clonase II (catalog no. 11791019). After recombination clones were selected and sequenced and deposited (Addgene 108685). For experiments using co-delivery of two plasmids, iRFP670-N1 (Addgene 45457) [43] was used.

### 2.6 Imaging and Analysis using HCS studio 2.0 Software

Images were acquired on an ArrayScan VTI HCA Reader (Thermo Fisher Scientific) using a 20x objective. For analysis, the Thermo Scientific AdvancedTargetValidationV4.1 application was used with the assay described in Figure S4.

### 2.7 *In vitro* nanoparticle mediated gene delivery

On the day of transfection, the old media was discarded and replaced with 40 μL of fresh RPE media. PBAE/pDNA nanoparticles were formed under optimal conditions previously described {Wilson, 2019 #907}. Briefly, pDNA was diluted in 25 mM magnesium acetate buffer ($MgAc_2$, pH 5) and aliquoted to individual wells on the right half of the 384-nanoparticle-source plate. End capped PBAEs from the left half of the 384 well round bottom source well place (Figure 2D) were then resuspended in parallel in 25 mM $MgAc_2$ using a ViaFlo microplate dispenser. After a brief centrifugation (1000 RCF for 1 minute) the solutions of unique PBAE structures were then transferred to the right half of the 384 well round bottom source well place containing pDNA (Figure 2D) in a 3:1 (vol/vol) ratio, resulting in a defined weight-weight (w/w) ratio between 20–100 of PBAE:DNA. The

nanoparticle source plate containing the PBAE/DNA mixtures was then briefly centrifuged (1000 RCF for 1 minute). To dispense nanoparticles to cells, 5 μL volumes of the NPs in each well were then added to the RPE monolayer (Figure 2E) and incubated with cells for 2 hours inside the 37°C incubator; all nanoparticles and media were then replaced with 50 μL of fresh RPE media. After approximately 48 hours to allow for reporter gene expression, images were acquired using an automated fluorescence-based imaging system (Cellomics ArrayScan VTI; Thermo Fisher Scientific) for nuclear-GFP and mCherry. Transfected cells were identified as those expressing both the endogenous nuclear GFP and exogenous mCherry reporters, and the percent of transfected cells, as well as cell viability, was determined for each NP and condition.

### 2.8 Immunostaining and Confocal Microscopy

iPS EP1 cells, without a nuclear-GFP reporter, were differentiated by plating them at 25,000 cells per $cm^2$ on Matrigel-coated borosilicate sterile 8-well chambered cover glasses (catalog no. 155409; Lab-Tek II; ) and allowed to grow for 25 days in RPE medium. On the day of transfection, the old media was discarded and replaced with 300 μL of fresh RPE media. The PBAE 5-3-J12 was then mixed with CAG-mCherry pDNA in a 3:1 (vol/vol) ratio, resulting in a defined weight-weight (w/w) ratio of 90:1 of PBAE:DNA. To dispense nanoparticles to cells, 50 μL volumes of the NPs containing 1500 ng DNA were then added to the RPE monolayer and incubated with cells for 2 hours inside the 37°C incubator; all nanoparticles and media were then replaced with 300 μL of fresh RPE media. After approximately 48 hours, to allow for reporter gene expression, the cells were fixed with 4% paraformaldehyde in PBS, cells were blocked and permeabilized for 30 min in 5% goat serum, 0.25% Triton X-100 in PBS, and then incubated for 1 h at room temperature with polyclonal mouse anti–ZO-1 (1/500; catalog no. 40–2200; Invitrogen) monoclonal rat anti–mCherry (1/1000; catalog no. M-11217; Molecular Probes). Cells were then incubated for 1 h at room temperature with the corresponding secondary antibody conjugated to Alexa 488 or Alexa 568 (Invitrogen), and counterstained with Hoechst 33342 (Invitrogen). Images were captured with a confocal microscope (Zeiss LSM 710).

### 2.9 Co-expression Assay

To assess the ability of top PBAE nanoparticles to co-deliver two plasmids, plasmids CAG-mCherry (Addgene 108685) and CMV-iRFP670 (Addgene 45457) [43] were diluted together in 25 mM $MgAc_2$ and used to form PBAE 5-3-J12 nanoparticles at a 90 w/w ratio. These nanoparticles were used to transfect a combined total DNA dose of 200 ng/well in 384 well plates. For the co-delivered condition, plasmids in 25 mM $MgAc_2$, were pre-mixed prior to complexation with PBAE and added to RPE monolayers together in the same nanoparticles. Transfection efficacy for iRFP and mCherry was then assessed 72 hours following transfection using the HCS assay as described.

### 2.10 Statistical analysis

Graph pad prism software (v.7.0) was used for data analysis. One-way ANOVA test was used for comparison of the results. For finding the differences between groups, data was analyzed by post-Hoc, Dunnett's multiple comparisons test. P values of ****p<.0001; ***p<.001; **p<.01; *p<.05 were considered as statistically significant.

# 3. RESULTS

## 3.1 Polymer Synthesis and Characterization

Four acrylate-terminated PBAEs that were shown previously to be effective for gene delivery in various cell types were synthesized as previously described [44] as neat polymers from small molecule diacrylate and amino monomers (Figure 1). The acrylate-terminated polymers were also washed twice with diethyl ether and characterized via gel permeation chromatography and $^{1}$H NMR to assess number average molecular weight ($M_N$) and to ensure that the majority of polymer molecules were acrylate terminated to allow for effective end-capping (Figure S1). The results indicated that all synthesized polymers, were acrylate terminated with number average molecular weights between 6.2 to 7.8 kDa (Figure S2). Precipitation in diethyl ether has previously been utilized to remove excess end-cap monomers reacted with base-polymers to avoid free monomer induced cytotoxicity [45]. We hypothesized that precipitation via diethyl ether even in the absence of end-cap monomers to be removed would increase molecular weight and reduce polydispersity of synthesized acrylate terminated polymers by removing oligomers that have been shown to be ineffective for gene delivery purposes [46, 47]. This effect was confirmed by GPC analysis of polymer before and after precipitation, whereby $M_N$ increased by an average of 41 ± 9% (mean ± SD) and PDI decreased by an average of 16 ± 9% (mean ± SD). The molecular weights of the base polymers are all within the optimal range for transfection efficacy previously reported for similar polymer structures [46].

Utilization of end-cap monomers in linear PBAEs has been demonstrated to greatly improve transfection efficacy compared to side-chain monomer terminated polymers (i.e. C32) [48–52]. Furthermore, polymer end-capping groups have been shown to significantly increase the efficacy of acrylate terminated base polymers that are almost entirely ineffective for both uptake and transfection [53]. With this rationale, we selected potential end-cap monomers from those previously published and available potential primary amine monomers from chemical supply companies. Polymer 4-4-Ac was end-capped with each potential monomer initially and pre-screened for transfection efficacy in HEK293T cells to separate out wholly ineffective end-cap monomers (Figure S3 and Table S4). From this pre-screen, we selected 36 end-cap monomers (Figure 1) to use for polymeric library preparation, having eliminated 24 of the structures for RPE screening tests.

The polymer nomenclature "$B_N$-$S_N$-XY" in the synthesized polymer library denotes base monomer (B) carbon number between acrylate moieties, and side-chain monomer (S) number denotes carbon number between hydroxyl as previously described.[44] Due to the large number of amino end-cap monomers, we utilized a new naming scheme whereby end-cap monomers were given a letter (J-P) for specific structural category (denoted X above) followed by a number for specific monomer in the category (denoted Y above). Structural categories of end-cap monomers included amino alkanes (J), amino piperidines (K), amino pyrollidines (L), amino alcohols (M), amino piperizines (N), diamino-ethers (O) and amino morpholinos (P). By this nomenclature, 3,3′-iminobis(N,N-dimethylpropylamine)-end terminated poly(1,5-pentanediol diacrylate-co-3 amino-1-propanol) (PBAE 5-3-J12) was

synthesized from monomers B5 and S3 to yield an acrylate terminated PBAE followed by end-capping with monomer J12 to yield a linear, end-capped polymer.

### 3.2 Polymer Library Preparation

The polymer library described above was prepared in a semi-automated, high-throughput manner to identify polymer formulations effective for transfection of iPSC derived RPE cells in a highly parallel manner as shown in Figure 2. For high-throughput polymer end-capping reactions, end-cap monomers in DMSO were distributed to deep-well 384-well plates, after which acrylate terminated polymers were distributed likewise in parallel and allowed to react for two hours at room temperature with gentle shaking. End-capped polymers in the master reaction plate were diluted further in DMSO and a set volume was distributed in parallel to individual nanoparticle source plates (384 well round-bottom plates). Nanoparticle source plates were then sealed and stored at −20°C with desiccant until the time of transfection. This method allowed many nanoparticle source plates to be prepared at one occasion to ensure reproducibility between transfections on different days.

### 3.3 High Throughput Semi-Automated NP Transfection to RPE Monolayers

To access the transfection efficacy of the PBAE nanoparticles in mature RPE monolayers at day 25 following seeding of differentiated RPE cells (Figure S5), we conducted a high throughput-screening assay with the prepared library of 148 PBAE structures. For high-throughput transfections, a nanoparticle source plate with polymers in one-half of the wells was thawed and DNA diluted in pH 5 magnesium acetate ($MgAc_2$) buffer was distributed to the right half of the plate. For initial screening assays we choose to use a plasmid in which expression of the fluorescent reporter mCherry is driven by the chicken $\beta$-actin with a CMV enhancer (CAG) promoter because the CAG promoter was previously shown to be highly active in human iPSC-derived RPE cells [54]. Each polymer was resuspended in pH 5 $MgAc_2$ buffer in parallel and mixed with the dilute DNA to form polyplex nanoparticles by electrostatic self-assembly. Nanoparticles were then distributed to plates of cells in parallel to screen for transfection efficacy using an image-based High Content Screening assay (Figure S4). This setup enabled 148 polymer structures per nanoparticle source plate to be tested with two replicates for each polymer per plate of cells.

Our library of polymers was first screened at a 60 w/w ratio of polymer to plasmid DNA to assess transfection efficacy (Figure 3A) and viability (Figure 3B) relative to untreated RPE monolayers. As previously observed, acrylate terminated polymers (5-3-Ac, etc) lacking any end-cap monomer failed to yield detectable transfection [55]. Heat map arrays of transfection efficacy demonstrated that more hydrophobic polymer structures (base polymers 5–3- and 4–5-) generally yielded greater transfection and the end-cap played an important role in the efficacy of polymers overall. Several leading PBAE structures, 5-3-J12, 5-3-O3 and 5-3-O4, resulted in 42%, 37% and, 34% positively transfected cells, respectively while maintaining high cell viability (90%, 97% and, 98%, respectively). Among all polymers evaluated, cell viability was not directly proportional to a polymer's ability to transfect RPE monolayers, as some other PBAEs demonstrated extremely low transfection efficacy despite high cell viability. Interestingly, the results of screening this library of polymers on mature RPE monolayers at day 25 post-seeding differed from transfection efficacy screening in

mitotic RPE cells on day 3 post-seeding (Figure S6), where more hydrophilic polymer structures demonstrated the highest efficacy and greater cytotoxicity was notable among all polymers. These results thus confirm our prior experience that polymer transfection efficiency can be highly cell type/state dependent and highlight the importance of optimizing polymers on the specific cell type and cell state of interest.

### 3.4 Validation of 5-3-J12 Nanoparticle Transfection Efficacy

In order to validate and optimize the top polymer structure identified in our screen, 5-3-J12, polymer to DNA w/w ratio and overall polymer dose per well were varied to identify optimal transfection conditions (Figure S7). With this optimization, 90 w/w 5-3-J12 nanoparticles were demonstrated to yield the greatest transfection efficacy (up to 60% transfection) compared to 30 w/w and 60 w/w nanoparticles of the same polymer structure at an equal polymer dose per well of cells. Assessment of a wide range of leading commercially available transfection reagents at multiple ratios of reagent to DNA and multiple DNA doses further demonstrated the enhanced efficacy of this new chemical compound in transfection of RPE monolayers (Figure S8). In direct comparisons, PBAE 5-3-J12 yielded statistically significantly higher transfection efficacy (Figure 4A) than all tested commercial transfection reagents as well as our previously developed top PBAE polymer for transfection of RPE cells (PBAE 557) [56]. Viability of RPE monolayers with nanoparticle 5-3-J12 was not statistically significantly different from untreated cells, in contrast to most commercial reagents, which induced significant cytotoxicity to achieve lower transfection efficacy (Figure 4B). PBAE 5-3-J12 further yielded a greater degree of transgene expression than the top commercial reagent ViaFect, as shown by both flow cytometry (Figure 4C) and by microscopy (Figure 4D). Overall transfection efficacy for all transfection reagents varied together across independently prepared iPSC-derivations of mature RPE monolayers over a 9-month time-span, but the top polymer structure, 5-3-J12, always yielded transfection efficiencies (20% to 60%) that were statistically higher than the top commercial reagent, ViaFect (Figure S9).

### 3.5 Biophysical Characterization of 5-3-J12 Nanoparticle

To further investigate the biophysical properties of 5-3-J12, we characterized these nanoparticles at multiple w/w ratios via dynamic light scattering (DLS), electrophoretic light scattering for zeta-potential, and nanoparticle tracking analysis (NTA). 5-3-J12 nanoparticles at w/w ratios of 30, 60 and 90 polymer to DNA varied significantly in diameter assessed by DLS and NTA with 90 w/w nanoparticles forming significantly smaller particles (Figure 5A,B). This result is consistent with our previously published findings that forming PBAE nanoparticles at high w/w ratios with excess polymer has a tendency to yield a smaller overall population of nanoparticles [57, 58]. Zeta-potential of 5-3-J12 did not vary with w/w ratio, with all 5-3-J12 nanoparticles measured to have a surface charge of between 25–30 mV (Figure 5C). The addition of the J12 end-cap moiety to base polymer 5-3-Ac was demonstrated to improve DNA binding capacity via a gel retention assay (Figure 5D), likely due to increased positive charge from the amine-containing J12 end-group. The diameter of PBAE 5-3-J12 nanoparticles assessed by TEM was similarly consistent with hydrodynamic diameter sizing measurements, showing dried particles of approximately 100 nm in diameter (Figure 5E).

### 3.6 Co-transfection and Properties of RPE Monolayer Transfected Cells

For *in vitro* mechanistic studies as well as potentially for *in vivo* ocular gene therapy applications, it could be advantageous to transfect cells simultaneously with multiple genes. We therefore tested whether our non-viral delivery system could provide efficient co-expression of multiple genes. Transfection of mature RPE monolayers with 5-3-J12 90 w/w nanoparticles prepared with CAG-mCherry and CMV-iRFP670 plasmids yielded up to 22% of cells showing co-expression of both genes (Figure 6A). Among cells detectably expressing either fluorescent protein, most showed expression of both genes (53.5 ± 1.4%), rather than expressing just one gene (15.0 ± 2.6% and 31.4 ± 2.7% for CAG-mCherry and CMV-iRFP670 respectively). In all transfection experiments, among the transfected cells we observed a wide range of expression levels. We also observed that there seemed to be a relationship between expression level and cell viability. With the strong synthetic CAG promoter, with both PBAE 5-3-J12 as well as ViaFect-mediated transfection, the cells that expressed the exogenous reporter genes at the highest levels were more likely to undergo cell death (see Supplementary Video that demonstrate time-lapse microscopy of highly expressing cells undergoing cell death for PBAE 5-3-J12 transfection (Video 1) and ViaFect transfection (Video 2)). However, the induction of cell death was determined not to be directly attributable to the polymers themselves as nanoparticles prepared with non-coding Cy5-labeled plasmid DNA [59] did not induce a significant level of cell death, whereas a reduction in the total number of nuclear-GFP positive cells per well for RPE monolayers transfected with the same nanoparticles prepared with the CAG-mCherry plasmid was observed (Figure S10). Finally, confocal microscopy assessment of RPE monolayers transfected and stained for tight junctions (ZO-1) at 48 hours post-transfection demonstrated the presence of tight junctions following transfection with 5-3-J12 (Figure 7).

## DISCUSSION

Safe and effective non-viral gene delivery of plasmid DNA to post-mitotic cells remains challenging in part due to the lack of nuclear membrane breakdown, which is a major barrier to gene delivery. Delivery of plasmid DNA to post-mitotic cells is of great utility for the study of retinal biology as well as for the development of non-viral therapeutic materials for retinal gene therapy. Here, we designed and utilized a semi-automated high throughput system to generate and identify candidate biodegradable polymer structures that mediate effective delivery to post-mitotic, mature RPE monolayers derived from induced pluripotent stem cells [38, 39]. While prior studies have utilized immortalized RPE cell lines such as ARPE-19 or hTERT-RPE1 to study gene delivery to RPE monolayers *in vitro*, these cell lines provide only a limited model of the cell behavior of RPE cells *in vivo* both in terms of cellular phenotype and gene expression profile. The ES-derived RPE monolayers used here have been previously validated to better mimic native RPE phenotype and gene expression of RPE cells in the human retina, enabling them to serve as a useful model for the study RPE biology in high throughput formats [39].

The approach for high throughput PBAE library generation described here is highly adaptable for rapid library generation and screening techniques. In contrast to prior automated and semi-automated synthesis libraries that have used pipetting robots such as

Tecan [60], our simplified semi-automated technique facilitates parallel testing of polymer structures that can be implemented with any parallel pipetting framework, including in 96 well plates with a simple multichannel pipet. Our approach also demonstrates the importance of end-cap monomer structure for determining the efficacy of linear PBAEs for transfection, an approach which is highly amenable to simple parallelization [52].

With these validated RPE monolayers and semi-automated polymer library preparation and screening technique, we identified multiple candidate polymer structures for transfection of post-mitotic RPE monolayers with the most promising candidate, 5-3-J12, yielding up to 60% transfection efficacy with minimal cytotoxicity. This polymer structure was further shown to enable co-delivery of two separate plasmids coding for two fluorescent proteins, and we demonstrated that tight junctions stained with anti-ZO-1 were still present at 48 hours post-transfection. The utilization of this screening approach is notable given that our prior candidate for transfection of RPE cells (PBAE 557), identified by screening in ARPE-19 monolayers [21], yields <15% transfection efficacy in our current assay with mature RPE monolayers. Similarly, widely-used commercial transfection reagents such as Lipofectamine 3000 and JetPRIME polyethylenimine were minimally effective at transfecting difficult-to-transfect post-mitotic RPE monolayers. The commercial reagent ViaFect was the most effective commercially available reagent tested, but it yielded less than half the level of transfection of our top identified polymer, PBAE 5-3-J12.

Our top identified polymer structure, a new composition that utilizes 3,3′-iminobis(N,N-dimethylpropylamine) as an end-group, was characterized as a nanoparticle and shown to possess biophysical properties very similar to other leading non-viral gene delivery particles (~100 nm in size with a positive surface charge). Given the relative ease of synthesis of PBAEs and their overall low cytotoxicty and permanence due to their rapid hydrolytic degradation rate [55], they represent a promising biological technology for routine *in vitro* transfections in the laboratory to further research into retinal biology and genetics.

Despite the promise of PBAEs for transfection of difficult to transfect cells, we do also want to mention a note of caution. Previous work has demonstrated that high levels of transgene expression, including high levels of fluorescent reporter protein expression, can induce apoptosis and other undesirable cellular changes in transfected cells, which may be a challenge for the use of high efficiency non-viral vectors such as those described in this manuscript [61]. Presumably related to this phenomenon, we did observe cellular changes and cell death in experiments in which RPE cells were induced to express high levels of mCherry here, a phenomenon that was not observed when using non-coding plasmid DNA. Potential approaches to limit the negatives effects of over-expression include utilization of self-limiting expression cassettes and use of weaker or regulatable promoters, as well as developing methods to directly reduce the cellular toxicity of over-expressed proteins.

## CONCLUSIONS

In summary, here we report the high-throughput screening and development of PBAE-based, biodegradable nanoparticles as efficient vehicles for delivering pDNA to human iPSC-RPE monolayers using a combinatorial chemistry approach. By screening a total of 140

synthesized PBAEs with varying chemical structures, we identified lead PBAE structures that resulted in markedly increased pDNA delivery efficiency *in vitro*. Our results suggest that PBAE can effectively complex pDNA into nanoparticles, and protect the pDNA from being degraded by environmental nucleases and deliver pDNA effectively to RPE monolayers. Furthermore, our results support our hypothesis that PBAE-mediated pDNA delivery efficiency can be modulated by tuning PBAE end group chemistry. Using human iPSC-RPE monolayers as model cell types, we identified several PBAE polymers that allow efficient pDNA delivery at levels that are double that of leading commercial transfection reagents, while maintaining high cell viability. The top synthetic polymer, 3,3′-iminobis(N,N-dimethylpropylamine)-end terminated poly(1,5-pentanediol diacrylate-co-3 amino-1-propanol) (5-3-J12), formed ~100 nm nanoparticles when mixed with plasmid DNA, could co-deliver multiple plasmids to human iPSC-RPE monolayers, and was capable of transfecting a majority of iPSC-RPE cells with minimal cytotoxicity. Together, our results highlight the promise of PBAE-based nanoparticles as novel non-viral gene carriers for pDNA delivery into hard-to-transfect cells such as RPE monolayers.

## Supplementary Material

Refer to Web version on PubMed Central for supplementary material.

## ACKNOWLEDGEMENTS

We are grateful to Baranda S. Hansen for technical assistance. The authors thank the Wilmer Microscopy and Imaging Core Facility (EY001765) at Johns Hopkins for use of their confocal microscopy.

FUNDING

This research was supported by grants from the Maryland Stem Cell Research Fund to D.J.Z. (EY027266), NIH grant (EY024249) to D.J.Z, BrightFocus Foundation to D.J.Z., RPB Nelson Trust Award for Retinitis Pigmentosa and unrestricted funds from Research to Prevent Blindness, Inc. to D.J.Z., generous gifts from the Guerrieri Family Foundation and from Mr. and Mrs. Robert and Clarice Smith to D.J.Z., Foundation Fighting Blindness to D.J.Z., Thome Foundation to D.J.Z., Beckman Foundation to D.J.Z., NSF Graduate Research Fellowships DGE-0707427 to DRW and DGE-1232825 to YR; the Bloomberg~Kimmel Institute for Cancer Immunotherapy to JJG; the NIH (R21EY026148, R01EB022148, R01CA228133, and the Wilmer Core Grant P30 EY001765); and a Research to Prevent Blindness / Dr. H. James and Carole Free Catalyst Award for Innovative Research Approaches for Age-Related Macular Degeneration to JJG.

## REFERENCES:

1. Trapani I and Auricchio A, Seeing the Light after 25 Years of Retinal Gene Therapy. Trends Mol Med, 2018. 24(8): p. 669–681. [PubMed: 29983335]
2. Kotterman MA and Schaffer DV, Engineering adeno-associated viruses for clinical gene therapy. Nature Reviews Genetics, 2014. 15(7): p. nrg3742.
3. Bitner H, et al., A homozygous frameshift mutation in BEST1 causes the classical form of Best disease in an autosomal recessive mode. Invest Ophthalmol Vis Sci, 2011. 52(8): p. 5332–8. [PubMed: 21467170]
4. den Hollander AI, et al., Leber congenital amaurosis: genes, proteins and disease mechanisms. Prog Retin Eye Res, 2008. 27(4): p. 391–419. [PubMed: 18632300]
5. Liu X, et al., Usherin is required for maintenance of retinal photoreceptors and normal development of cochlear hair cells. Proc Natl Acad Sci U S A, 2007. 104(11): p. 4413–8. [PubMed: 17360538]
6. Baum C, et al., Mutagenesis and oncogenesis by chromosomal insertion of gene transfer vectors. Hum Gene Ther, 2006. 17(3): p. 253–63. [PubMed: 16544975]

7. Wright JF, Manufacturing and characterizing AAV-based vectors for use in clinical studies. Gene therapy, 2008. 15(11): p. 840. [PubMed: 18418418]
8. Asokan A, Schaffer DV, and Samulski RJ, The AAV vector toolkit: poised at the clinical crossroads. Molecular Therapy, 2012. 20(4): p. 699–708. [PubMed: 22273577]
9. Oliveira AV, Rosa da Costa AM, and Silva GA, Non-viral strategies for ocular gene delivery. Mater Sci Eng C Mater Biol Appl, 2017. 77: p. 1275–1289. [PubMed: 28532005]
10. Boylan NJ, et al., Enhancement of airway gene transfer by DNA nanoparticles using a pH-responsive block copolymer of polyethylene glycol and poly-L-lysine. Biomaterials, 2012. 33(7): p. 2361–71. [PubMed: 22182747]
11. Cheng W, et al., Delivery of a granzyme B inhibitor gene using carbamate-mannose modified PEI protects against cytotoxic lymphocyte killing. Biomaterials, 2013. 34(14): p. 3697–705. [PubMed: 23422590]
12. de la Fuente M, et al., Chitosan-based nanostructures: a delivery platform for ocular therapeutics. Adv Drug Deliv Rev, 2010. 62(1): p. 100–17. [PubMed: 19958805]
13. Kim TH, et al., Galactosylated chitosan/DNA nanoparticles prepared using water-soluble chitosan as a gene carrier. Biomaterials, 2004. 25(17): p. 3783–92. [PubMed: 15020154]
14. Read ML, et al., A versatile reducible polycation-based system for efficient delivery of a broad range of nucleic acids. Nucleic Acids Res, 2005. 33(9): p. e86. [PubMed: 15914665]
15. Wang H, Shi HB, and Yin SK, Polyamidoamine dendrimers as gene delivery carriers in the inner ear: How to improve transfection efficiency. Exp Ther Med, 2011. 2(5): p. 777–781. [PubMed: 22977574]
16. Yu H, Russ V, and Wagner E, Influence of the molecular weight of bioreducible oligoethylenimine conjugates on the polyplex transfection properties. AAPS J, 2009. 11(3): p. 445–55. [PubMed: 19504187]
17. Hornstein BD, et al., Effects of Circular DNA Length on Transfection Efficiency by Electroporation into HeLa Cells. PLoS One, 2016. 11(12): p. e0167537. [PubMed: 27918590]
18. Vaughan EE, DeGiulio JV, and Dean DA, Intracellular trafficking of plasmids for gene therapy: mechanisms of cytoplasmic movement and nuclear import. Current gene therapy, 2006. 6(6): p. 671–681. [PubMed: 17168698]
19. Bishop CJ, et al., Quantification of cellular and nuclear uptake rates of polymeric gene delivery nanoparticles and DNA plasmids via flow cytometry. Acta Biomaterialia, 2016. 37: p. 120–130. [PubMed: 27019146]
20. Yang F, et al., Gene delivery to human adult and embryonic cell-derived stem cells using biodegradable nanoparticulate polymeric vectors. Gene Ther, 2009. 16(4): p. 533–46. [PubMed: 19129861]
21. Sunshine JC, et al., Poly(beta-amino ester)-nanoparticle mediated transfection of retinal pigment epithelial cells in vitro and in vivo. PLoS One, 2012. 7(5): p. e37543. [PubMed: 22629417]
22. Strauss O, The retinal pigment epithelium in visual function. Physiol Rev, 2005. 85(3): p. 845–81. [PubMed: 15987797]
23. Rodrigues GA, et al., Pharmaceutical Development of AAV-Based Gene Therapy Products for the Eye. Pharm Res, 2018. 36(2): p. 29. [PubMed: 30591984]
24. McClements ME and MacLaren RE, Adeno-associated Virus (AAV) Dual Vector Strategies for Gene Therapy Encoding Large Transgenes. Yale J Biol Med, 2017. 90(4): p. 611–623. [PubMed: 29259525]
25. Moore NA, et al., Gene therapy for inherited retinal and optic nerve degenerations. Expert Opin Biol Ther, 2018. 18(1): p. 37–49. [PubMed: 29057663]
26. Planul A and Dalkara D, Vectors and Gene Delivery to the Retina. Annu Rev Vis Sci, 2017. 3: p. 121–140. [PubMed: 28937950]
27. Abul-Hassan K, Walmsley R, and Boulton M, Optimization of non-viral gene transfer to human primary retinal pigment epithelial cells. Curr Eye Res, 2000. 20(5): p. 361–6. [PubMed: 10855030]
28. Bejjani RA, et al., Nanoparticles for gene delivery to retinal pigment epithelial cells. Mol Vis, 2005. 11: p. 124–32. [PubMed: 15735602]

29. Chaum E, Hatton MP, and Stein G, Polyplex-mediated gene transfer into human retinal pigment epithelial cells in vitro. J Cell Biochem, 1999. 76(1): p. 153–60. [PubMed: 10581009]
30. Jayaraman MS, et al., Nano chitosan peptide as a potential therapeutic carrier for retinal delivery to treat age-related macular degeneration. Mol Vis, 2012. 18: p. 2300–8. [PubMed: 22977298]
31. Liu HA, et al., A lipid nanoparticle system improves siRNA efficacy in RPE cells and a laser-induced murine CNV model. Invest Ophthalmol Vis Sci, 2011. 52(7): p. 4789–94. [PubMed: 21519028]
32. Mannermaa E, et al., Long-lasting secretion of transgene product from differentiated and filter-grown retinal pigment epithelial cells after nonviral gene transfer. Curr Eye Res, 2005. 30(5): p. 345–53. [PubMed: 16020265]
33. Mannisto M, et al., The role of cell cycle on polyplex-mediated gene transfer into a retinal pigment epithelial cell line. J Gene Med, 2005. 7(4): p. 466–76. [PubMed: 15619286]
34. Mannisto M, et al., Structure-activity relationships of poly(L-lysines): effects of pegylation and molecular shape on physicochemical and biological properties in gene delivery. J Control Release, 2002. 83(1): p. 169–82. [PubMed: 12220848]
35. Peeters L, et al., Post-pegylated lipoplexes are promising vehicles for gene delivery in RPE cells. J Control Release, 2007. 121(3): p. 208–17. [PubMed: 17630013]
36. Peng CH, et al., Delivery of Oct4 and SirT1 with cationic polyurethanes-short branch PEI to aged retinal pigment epithelium. Biomaterials, 2011. 32(34): p. 9077–88. [PubMed: 21890195]
37. Bishop CJ, et al., The effect and role of carbon atoms in poly(beta-amino ester)s for DNA binding and gene delivery. J Am Chem Soc, 2013. 135(18): p. 6951–7. [PubMed: 23570657]
38. Maruotti J, et al., A simple and scalable process for the differentiation of retinal pigment epithelium from human pluripotent stem cells. Stem Cells Transl Med, 2013. 2(5): p. 341–54. [PubMed: 23585288]
39. Maruotti J, et al., Small-molecule-directed, efficient generation of retinal pigment epithelium from human pluripotent stem cells. Proc Natl Acad Sci U S A, 2015. 112(35): p. 10950–5. [PubMed: 26269569]
40. Gamm DM, et al., A novel serum-free method for culturing human prenatal retinal pigment epithelial cells. Invest Ophthalmol Vis Sci, 2008. 49(2): p. 788–99. [PubMed: 18235029]
41. Wilson DR and Green JJ, Nanoparticle Tracking Analysis for Determination of Hydrodynamic Diameter, Concentration, and Zeta-Potential of Polyplex Nanoparticles, in Biomedical Nanotechnology. 2017, Springer. p. 31–46.
42. Tzeng SY, et al., Polymeric nanoparticle-based delivery of TRAIL DNA for cancer-specific killing. Bioeng Transl Med, 2016. 1(2): p. 149–159. [PubMed: 28349127]
43. Shcherbakova DM and Verkhusha VV, Near-infrared fluorescent proteins for multicolor in vivo imaging. Nature Methods, 2013. 10: p. 751. [PubMed: 23770755]
44. Tzeng SY, et al., Non-viral gene delivery nanoparticles based on poly(β-amino esters) for treatment of glioblastoma. Biomaterials, 2011. 32(23): p. 5402–10. [PubMed: 21536325]
45. Green JJ, et al., Nanoparticles for gene transfer to human embryonic stem cell colonies. Nano letters, 2008. 8(10): p. 3126–30. [PubMed: 18754690]
46. Eltoukhy AA, et al., Effect of molecular weight of amine end-modified poly(β-amino ester)s on gene delivery efficiency and toxicity. Biomaterials, 2012. 33(13): p. 3594–603. [PubMed: 22341939]
47. Bishop CJ, et al., The effect and role of carbon atoms in poly(β-amino ester)s for DNA binding and gene delivery. Journal of the American Chemical Society, 2013. 135(18): p. 6951–7. [PubMed: 23570657]
48. Zugates GT, et al., Rapid optimization of gene delivery by parallel end-modification of poly (β-amino ester) s. Molecular Therapy, 2007. 15(7): p. 1306–1312.
49. Anderson DG, Lynn DM, and Langer R, Semi-automated synthesis and screening of a large library of degradable cationic polymers for gene delivery. Angewandte Chemie (International ed. in English), 2003. 42(27): p. 3153–8. [PubMed: 12866105]
50. Akinc A, et al., Synthesis of poly (β-amino ester) s optimized for highly effective gene delivery. Bioconjugate chemistry, 2003. 14(5): p. 979–988. [PubMed: 13129402]

51. Green JJ, et al., Combinatorial Modification of Degradable Polymers Enables Transfection of Human Cells Comparable to Adenovirus. Advanced Materials, 2007. 19(19): p. 2836–2842.
52. Sunshine J, et al., Small-Molecule End-Groups of Linear Polymer Determine Cell-type Gene-Delivery Efficacy. Advanced Materials, 2009. 21(48): p. 4947–4951. [PubMed: 25165411]
53. Sunshine JC, Peng DY, and Green JJ, Uptake and transfection with polymeric nanoparticles are dependent on polymer end-group structure, but largely independent of nanoparticle physical and chemical properties. Molecular pharmaceutics, 2012. 9(11): p. 3375–83. [PubMed: 22970908]
54. Cereso N, et al., Proof of concept for AAV2/5-mediated gene therapy in iPSC-derived retinal pigment epithelium of a choroideremia patient. Mol Ther Methods Clin Dev, 2014. 1: p. 14011. [PubMed: 26015956]
55. Sunshine JC, et al., Effects of base polymer hydrophobicity and end-group modification on polymeric gene delivery. Biomacromolecules, 2011. 12(10): p. 3592–600. [PubMed: 21888340]
56. Sunshine JC, et al., Poly(β-amino ester)-nanoparticle mediated transfection of retinal pigment epithelial cells in vitro and in vivo. PloS one, 2012. 7(5): p. e37543–e37543. [PubMed: 22629417]
57. Kozielski KL, et al., Bioreducible cationic polymer-based nanoparticles for efficient and environmentally triggered cytoplasmic siRNA delivery to primary human brain cancer cells. ACS nano, 2014. 8(4): p. 3232–41. [PubMed: 24673565]
58. Wilson DR, et al., Continuous microfluidic assembly of biodegradable poly(beta-amino ester)/DNA nanoparticles for enhanced gene delivery. J Biomed Mater Res A, 2017. 105(6): p. 1813–1825. [PubMed: 28177587]
59. Wilson DR, et al. Development of a pH Sensor to Probe Endosomal Buffering of Polymeric Nanoparticles Effective for Gene Delivery. 2016. Molecular Therapy.
60. Anderson DG, et al., A polymer library approach to suicide gene therapy for cancer. Proceedings of the National Academy of Sciences of the United States of America, 2004. 101(45): p. 16028–16033. [PubMed: 15520369]
61. Liu H-S, et al., Is green fluorescent protein toxic to the living cells? Biochemical and biophysical research communications, 1999. 260(3): p. 712–717. [PubMed: 10403831]

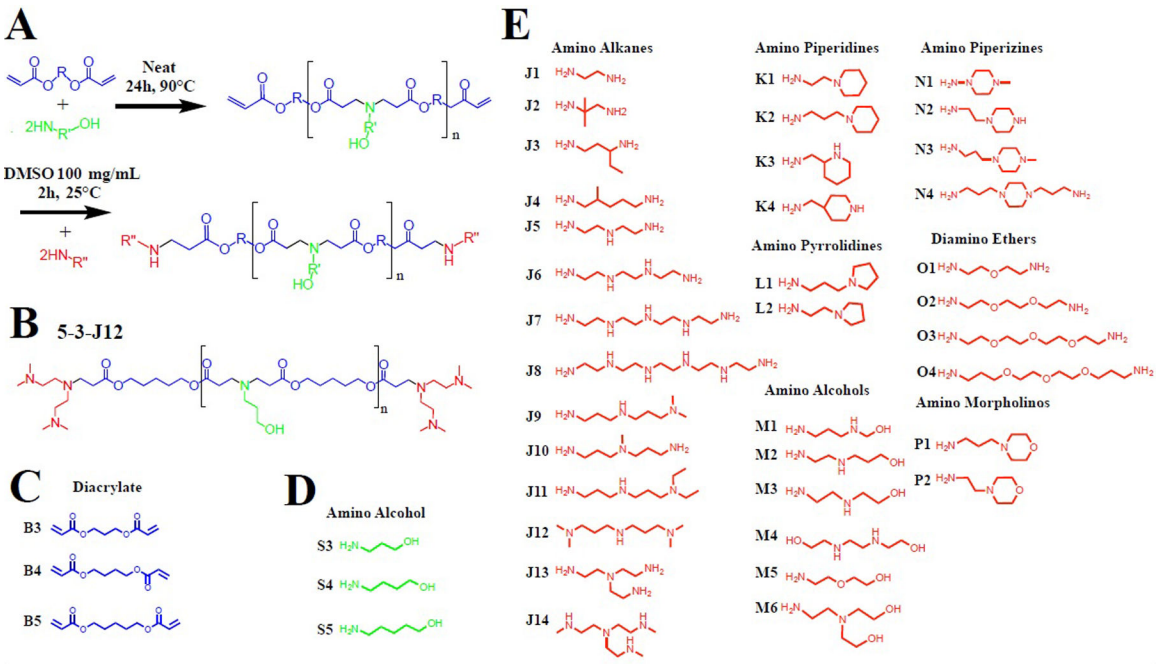


**Figure 1. Sequential poly(beta-amino ester)s (PBAEs) library construction and synthesis scheme**

**(A)** Synthesis scheme of linear PBAEs from diacrylate and primary amine small monomers to yield acrylate terminated polymers, followed by end-capping to yield linear end-capped PBAEs. **(B)** Representative PBAE 5-3-J12 formed from monomers B5, S3 and end-cap J12. **(C)** Three diacrylate monomers and **(D)** three side-chain amino alcohols utilized in library synthesis. **(E)** 36 end-cap monomers identified as effective for transfection.

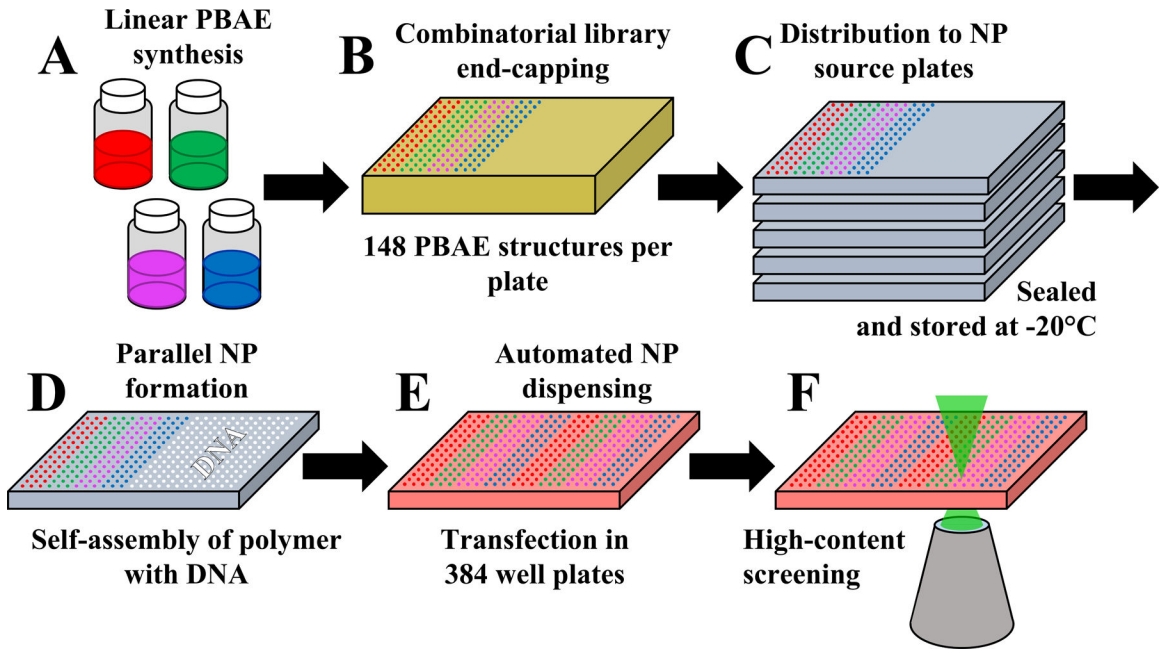


**Figure 2. Schematic of combinatorial PBAE library construction**

**(A)** Linear base polymer PBAEs were synthesized in vials to be acrylate terminated, then characterized via 1H NMR and GPC **(B)** Synthesized acrylate-terminated polymers were dispensed into a 384 well round bottom plate using a ViaFlo 96/384 microplate dispenser and end-capped with respective end-cap monomers. A total of 4 different base polymers as shown in different color scheme were end-capped per master plate containing 36 end-cap monomers each. **(C)** Source plates were then replicated from one master plate and stored them at −80 °C for future use. **(D)** End capped linear polymers (left 12 columns of the plate) were mixed with plasmid DNA (right 12 columns of the plate) to formulate NPs. **(E)** The RPE monolayers were transfected using an automated Viaflo microplate dispenser and incubated for 2 hours with NPs. **(F)** Images were captured using Cellomics.

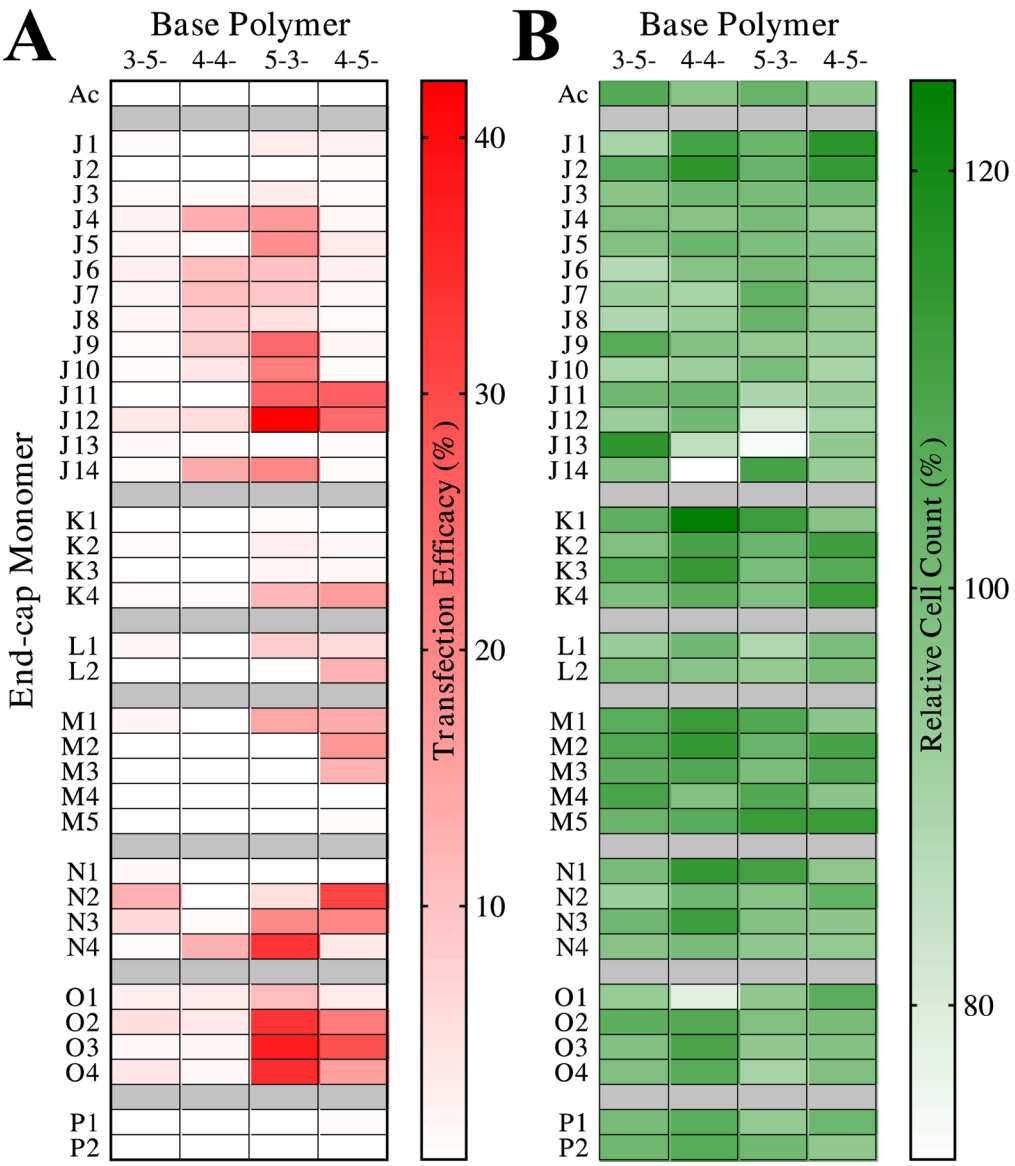


**Figure 3: High throughput screening of PBAE nanoparticles in confluent D25 RPE monolayers.**

**(A)** Heat maps showing the percentage transfected RPE cells and **(B)** relative percentage survival rate following the introduction of 148 different nanoparticles to confluent RPE monolayers at day 25 post seeding using a 60 w/w ratio of polymer to CAG-mCherry plasmid DNA. The color scale bar refers to the percentage transfection efficiency and percentage survival that was calculated based on the number of mCherry positive cells detected from the total cell population. Transfection efficacy and relative cell count were assessed approximately 48 hours after adding nanoparticles to cells.

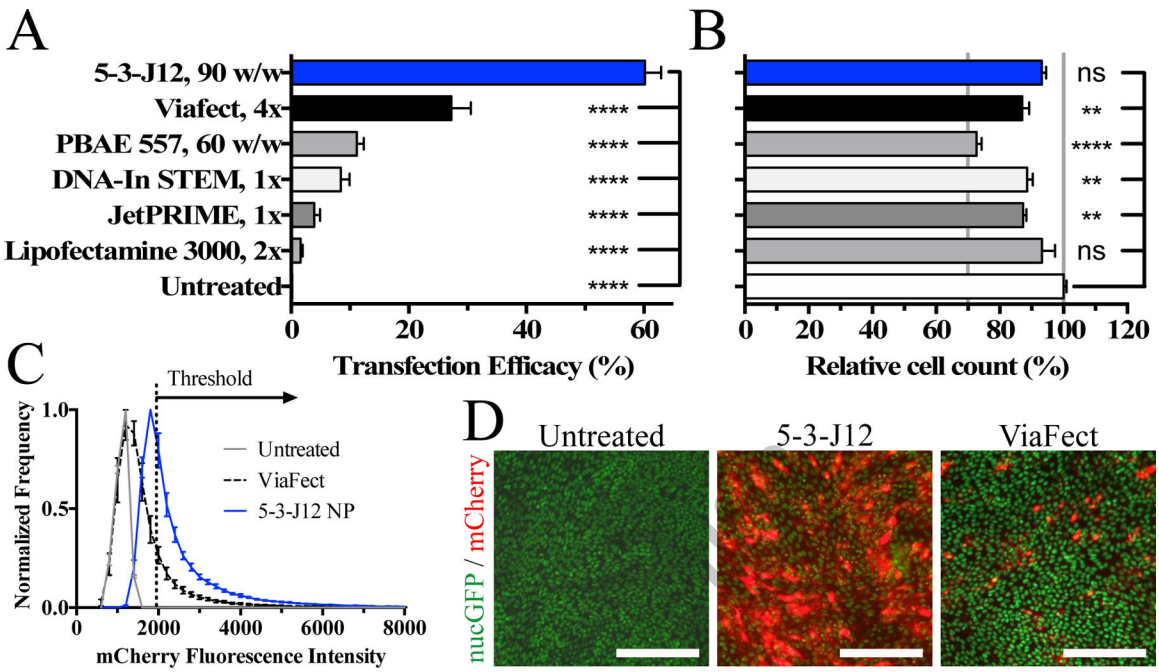


**Figure 4: Transfection of RPE monolayers with top PBAE nanoparticles and with commercially available reagents.**

**(A)** Transfection efficacy and **(B)** relative cell count of optimized nanoparticle formulation compared to commercial reagents. (One-way ANOVA with Dunnett corrected multiple comparisons) assessed approximately 72 hours after adding reagents to cells. **(C)** Relative expression level of cells transfected with 5-3-J12 and ViaFect demonstrating a greater number of cells expressing at all levels of expression. **(D)** Representative microscope images of RPE cells expressing nuclear GFP (green) and transfected with mCherry (red). Scale bar is 100 μm. Bars show mean ± SEM of four wells.

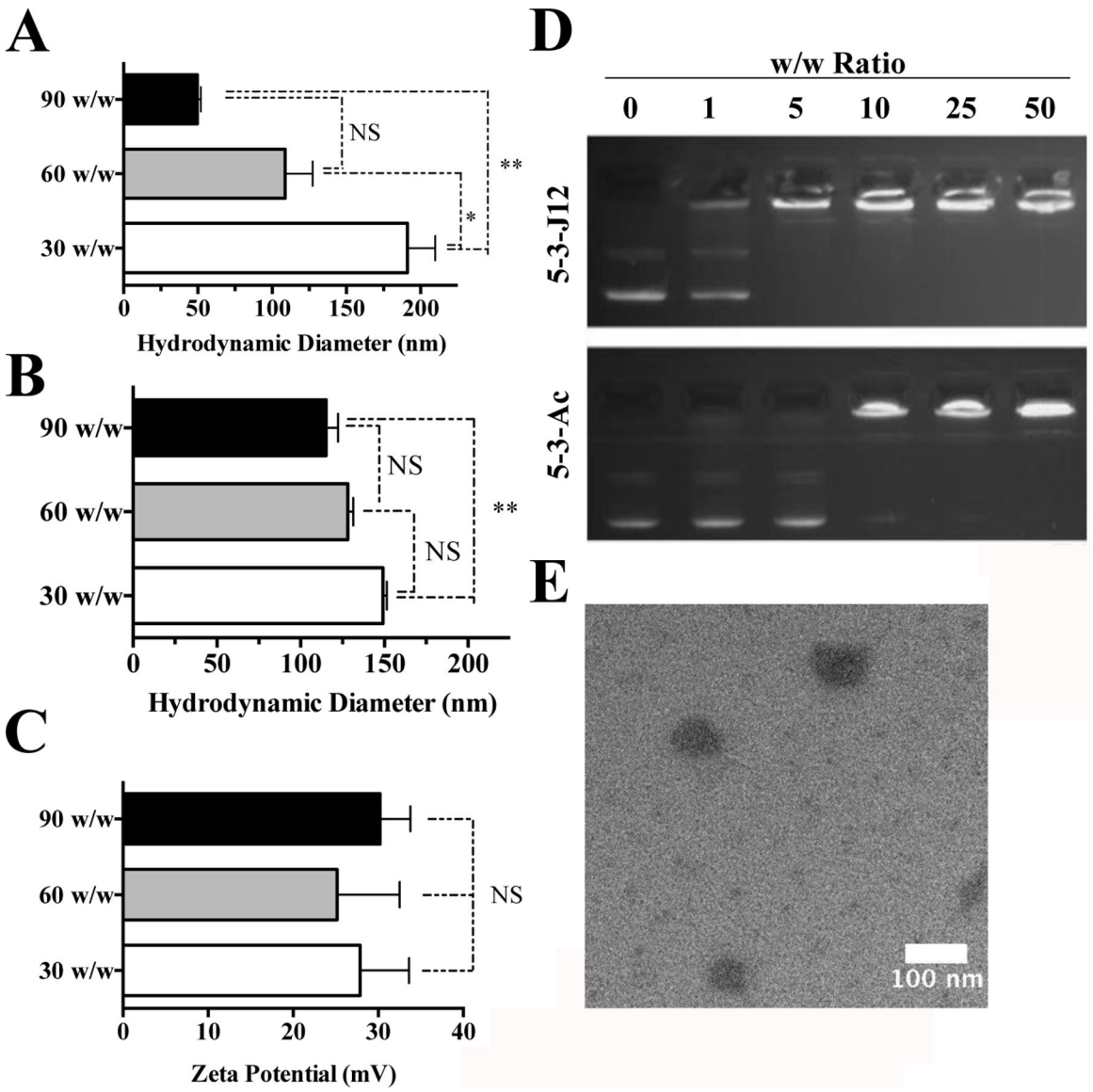


**Figure 5: PBAE 5-3-J12/DNA Nanoparticle Characterization**

**(A)** Nanoparticle hydrodynamic diameter measurements assessed via DLS z-average and **(B)** NTA showed that average diameter decreased as polymer: DNA w/w ratio increased. DLS z-average measurements were statistically lower for 90 w/w nanoparticles, compared to 30 w/w nanoparticles. **(C)** Nanoparticle zeta-potential did not statistically differ between the nanoparticles at different w/w ratios. **(D)** End-capping with monomer J12 improved DNA binding compared to acrylate-terminated polymers. PBAE 5-3-J12 fully retarded DNA at w/w ratios down to 5 w/w, in contrast to the acrylate terminated polymer, which was only effective down to a 10 w/w ratio. **(E)** TEM showed 5-3-J12/DNA nanoparticles have a spherical morphology and size of approximately 100 nm. Graphs show the mean of three independently prepared samples. *$p < 0.01$, **$p < 0.001$, based on one-way ANOVA with Tukey's *post hoc* test.

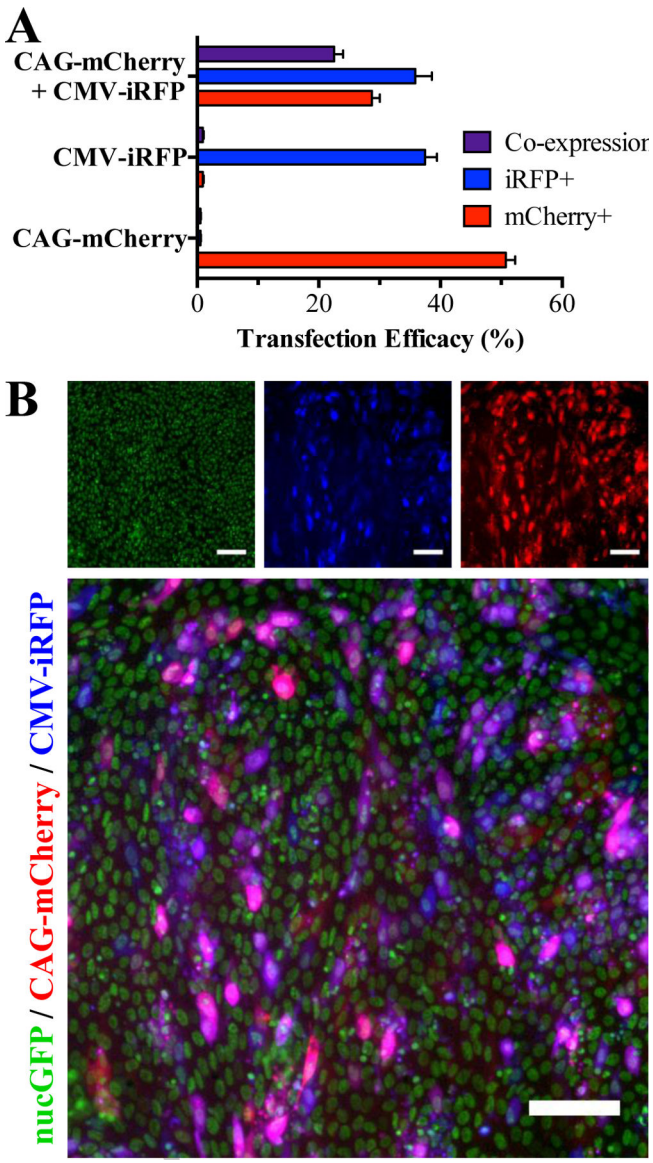


**Figure 6: Co-transfection of two reporter plasmids with PBAE 5-3-J12/DNA nanoparticles.**

(A) Nanoparticles formed with pre-mixed plasmids encoding CAG-mCherry and CMV-iRFP enabled RPE monolayers to co-express two exogenous genes simultaneously when assessed at approximately 72 hours post addition of nanoparticles. The majority of the cell population detectable as expressing either fluorescent protein, expressed both fluorescent proteins. (B) Representative RPE monolayers co-transfected with both CAG-mCherry (red) CMV-iRFP670 (blue) reporter constructs. A purple color indicates co-expression of the two exogenous genes. Scale bar is 100 μm. Bars show mean ± SEM of four wells.

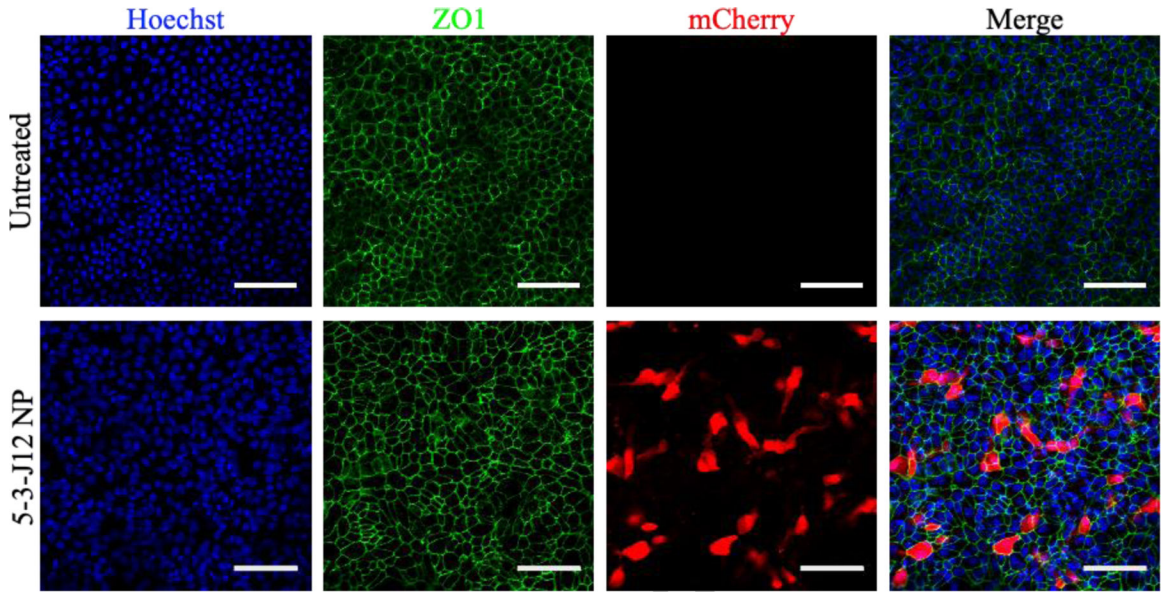


**Figure 7: RPE monolayer morphology after transfection.**

RPE monolayers were fixed and stained for tight junction protein ZO-1 to assess morphology of cells following transfection. Monolayers transfected with −3-J12/DNA nanoparticles at a 90 w/w ratio to express mCherry had ZO-1 present at cell boundaries but overall cell morphology differed from untreated cells. Scale bar is 50 μm.